Telematics data for geospatial and temporal mapping of urban mobility

Ghaffarpasand, Omid; Pope, Francis D

DOI:
10.1016/j.scitotenv.2023.164940

Document Version
Publisher's PDF, also known as Version of record

Citation for published version (Harvard):
Ghaffarpasand, O & Pope, FD 2023, 'Telematics data for geospatial and temporal mapping of urban mobility: Fuel consumption, and air pollutant and climate-forcing emissions of passenger cars', *Science of the Total Environment*, vol. 894, 164940. https://doi.org/10.1016/j.scitotenv.2023.164940

Science of the Total Environment 894 (2023) 164940

Contents lists available at ScienceDirect

Science of the Total Environment

journal homepage: www.elsevier.com/locate/scitotenv

Telematics data for geospatial and temporal mapping of urban mobility: Fuel consumption, and air pollutant and climate-forcing emissions of passenger cars

Omid Ghaffarpasand, Francis D. Pope *

School of Geography, Earth, and Environmental Sciences, University of Birmingham, Birmingham, UK

HIGHLIGHTS

- We use GeoSTMUM here to estimate vehicle dynamics with high spatiotemporal resolution.
- Telematics data were collected from the West Midlands in the UK for 2016 and 2018.
- Real-urban FC and EFs are estimated by vehicle dynamics and real-world measurements.
- Fleet renovation reduces real-urban NOx EFs by over 14 % for the studied period.
- Road slope has an increasing impact of 2–5 % on the estimated real-urban FC and EFs.

GRAPHICAL ABSTRACT

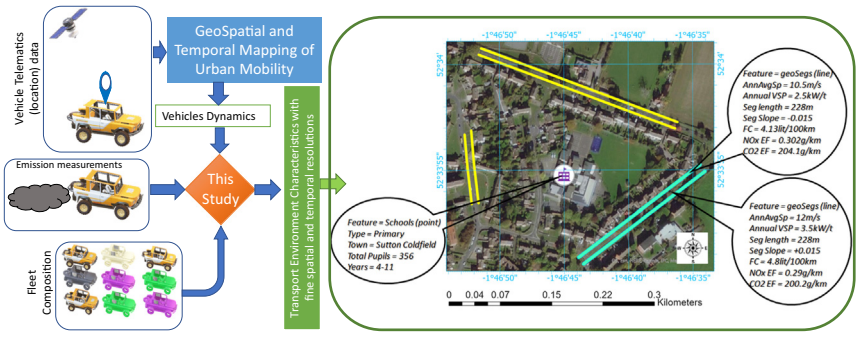

ARTICLE INFO

Editor: Pavlos Kassomenos

Keywords:
GeoST mapping of urban mobility
Road transport
Vehicular emissions
Telematics
Fuel consumption
Fleet renovation

ABSTRACT

In this study, we use the approach of geospatial and temporal (GeoST) mapping of urban mobility to evaluate the speed-time-acceleration profile (dynamic status) of passenger cars. We then use a pre-developed model, fleet composition and real-world emission factor (EF) datasets to translate vehicles dynamics status into real-urban fuel consumption (FC) and exhaustive (CO_2 and NO_x) emissions with high spatial (15 m) and temporal (2 h) resolutions. Road transport in the West Midlands, UK, for 2016 and 2018 is the spatial and temporal scope of this study. Our approach enables the analysis of the influence of factors such as road slope, non-rush/rush hour and weed days/weekends effects on the characteristics of the transport environment. The results show that real-urban NO_x EFs reduced by more than 14 % for 2016–18. This can be attributed to the increasing contribution of Euro 6 vehicles by 63 %, and the increasing contribution of diesel vehicles by 13 %. However, the variations in the real-urban FC and CO_2 EFs are less significant (±2 %). We found that the FC estimated for driving under the NEDC (National European Driving Cycle) is a qualified benchmark for evaluating real-urban FCs. Considering the role of road slope increases the estimated real-urban FC, and NO_x, and CO_2 EFs by a weighted average of 4.8 %, 3.9 %, and 3.0 %, respectively. Time of travel (non-rush/rush hour or weed days/weekends) has a profound effect on vehicle fuel consumption and related emissions, with EFs increasing in more free-flowing conditions.

1. Introduction

The transportation of individuals, services and goods, is a key pillar of social welfare, economic growth, and development (Pradhan, 2019). For example, within the European Union (EU), the transportation sector provides 5 % of employment and contributes over 9 % of the gross value added (EU, 2019). The internal combustion engine is currently still the dominant form of propulsion system used by road vehicles, with road transportation being one of the largest consumers of petrochemical fuel worldwide, responsible for around 29 % of global energy use in 2018 (Chen et al., 2016). The combustion of this fuel is responsible for around a quarter

* Corresponding author.
E-mail address: f.pope@bham.ac.uk (F.D. Pope).

http://dx.doi.org/10.1016/j.scitotenv.2023.164940
Received 17 February 2023; Received in revised form 25 May 2023; Accepted 14 June 2023
Available online 19 June 2023

of global carbon dioxide (CO_2) emissions (Zhang et al., 2018), and hence transport is a key cause of climate change (Wang et al., 2019). Gaseous and particulate matter pollutants are also produced through the combustion process, hence road transport contributes significantly to air pollution, especially with respect to nitrogen oxides (NO_x), see for example Ghaffarpasand et al. (2020b) and Coelho et al. (2022).

A deep understanding of vehicular emissions and fuel consumption is a vital prerequisite for any emission mitigation strategy. Vehicular emission factors (EFs) and emission rates (ERs) provide the emitted mass of pollutants per distance travelled and per travel time, respectively. The emission performance of different vehicle subsets, under real-world or controlled/laboratory conditions, can be assessed by different methods. Portable emission measurement systems (PEMS) and vehicle emission remote sensing systems (VERSS) are used to analyse real-world EFs (Ghaffarpasand et al., 2020a; Ghaffarpasand et al., 2020d), and dynamometers are frequently applied to assess EFs under controlled conditions (Liu et al., 2017). Fuel consumption (FC) of moving vehicles is usually estimated by the real-world measurement of instantaneous CO_2 ER. The FC can then be calculated through the method of carbon balance (Ghaffarpasand et al., 2021; Hu et al., 2012; Zhang et al., 2014b). An alternative methodology is to link FC to vehicle dynamic status, i.e., engine power, over a range of driving conditions (Borken-Kleefeld et al., 2018; Davison et al., 2020; Hausberger, 2003). The relationships between the vehicle dynamic status and the instantaneous EFs, ERs and FCs have been detailed by Davison et al. (2020) and Grange et al. (2019).

Driving cycles (DCs) were one of the first attempts to understand vehicle dynamics status, through the provision of speed-time-acceleration information (Hu et al., 2022; Hung et al., 2007; Soto et al., 2023). A wide body of research details the methods and techniques of developing DCs and their wide applications in transportation and freight logistics, see for example Bhatti et al. (2021) and Marabete et al. (2022). DCs are usually developed using a small volume of data collected from a few GPS-connected vehicles that are monitored over certain routes and times. Hence, the spatial and temporal resolutions of DCs are typically limited. Data collection over large road networks is difficult with DCs due to time and budget constraints. DCs do not include detailed information on spatial and temporal factors such as road type, road slope, time of travel effects, and hence these important factors cannot be included in the analysis of vehicle dynamic status (Kancharla and Ramadurai, 2018). Previously, the effect of road slope upon the emission performance and FC of on-road vehicles has been shown to be significant (Jia et al., 2021; Molina Campoverde et al., 2022.

Vehicle telematics data provide information on the timestamped positions of vehicles and are a promising data source with which to address the shortage of road data (Ghaffarpasand et al., 2022). Typically, telematics data are collected from GPS-connected vehicles whose drivers achieve fairer pricing in their car insurance premia in exchange for sharing their data. Telematics data are also used for freight logistics support, driving behaviour assessment, and traffic flow analysis in the transportation industries (Huang and Meng, 2019; Walker and Manson, 2014).

Vehicle telematics data are used within Satellite Navigation (satnav) services such as Google Maps or Waze to improve best route calculations. These services calculate the average speeds along connected links between pairs of destinations as well as using traffic forecasts, incident reports and other cognate information. Recently, Google in cooperation with US National Renewable Energy Laboratory (NREL) developed an eco-friendly routing algorithm to estimate the fuel consumption of a vehicle for any given route across road segments and driving conditions (Google Maps, 2023). The algorithm receives the vehicle engine type, i.e. petrol, diesel, hybrid or electric, and estimates the fuel consumption using factors such as the average fuel or energy consumption for vehicles in the studied region, steepness of hills in the route, stop-and-go traffic patterns, and road types. Currently, these services do not deliver any information on the vehicle's dynamic status, i.e., speed-acceleration-variation profiles. Also, they do not allow interrogation of historic data, which precludes their use in transport planning and policy-making.

Previously, vehicle GPS data has been used in transport planning studies or vehicle emission estimations. For example, Chen et al. (2016) estimated traffic volume from vehicle GPS and then estimated the corresponding NO_x concentration using a non-linear optimisation model. Gately et al. (2017) estimate the road EFs using detailed hourly vehicle speeds to develop the vehicular emission inventory of Eastern Massachusetts, Boston, US. Ghaffarpasand et al. (2020c) used GPS data of test vehicles to develop a local DC, with corresponding road EFs, and then developed a vehicular emission inventory for the city of Isfahan, Iran. A similar approach by Ibarra-Espinosa et al. (2020) developed a vehicular emission inventory for southeast Brazil. Mjøsund and Hovi (2022) used vehicle GPS data to study the freight vehicle activities in seven Norwegian cities.

Recently, Ghaffarpasand and Pope, 2023) propose a new approach of 'geospatial and temporal (GeoST) mapping of urban mobility' to translate vehicle telematics data into urban mobility characteristics at high geospatiotemporal resolutions (15 m and 2 h spatial and temporal scales, respectively). This approach provides a detailed understanding of the speed-acceleration profiles from which the vehicle-specific power (VSP) can be estimated. When calculated as a function of speed and acceleration, VSP is found to be a highly informative metric to estimate vehicle emissions and fuel consumption (Jiménez, 1998).

In this study, we provide a new approach for converting vehicle telematics data into estimates of vehicular emissions and fuel consumption over different spatial and temporal scales. We combine GeoST mapping of urban mobility with comprehensive datasets of fleet composition and real-world vehicle emissions to define new geospatial attributes of fuel consumption and vehicle emissions. In this new paradigm, fuel consumption and vehicular emissions are parameterized as urban features and can be analysed within geospatial frameworks, along with other urban features that can affect driving behaviour.

2. Material and methods

2.1. Vehicle telematics data, data description

We use vehicle telematics data provided by a UK-based telematics company, the Floow (www.thefloow.com). The data, which were instantaneous speed-time data, were collected from passenger cars, vehicles 3.885 tons or less (EU_Commission, 1999), for their journeys on the roads. Data is first QC/QA checked by the company, anonymised, and then aggregated by road sections and time bins in compliance with the EU and UK General Data Protection Regulation (GDPR). The aggregated data are subdivided into segments with specific geospatial and temporal characteristics (hereafter called GeoST-segments), and then the speed-acceleration-frequency-distribution (SAFD) matrix is calculated for each GeoST-segment. Essentially, GeoST-segments are geospatial polyline features with time-specific assignments aligned along the direction of traffic flow. SAFD is a normalised matrix that shows the speed and acceleration distribution of cars in each GeoST-segment. The average speed and acceleration are estimated using the SAFD matrix. This approach is called GeoSpatial and Temporal (GeoST) Mapping of Urban Mobility and is discussed in detail by Ghaffarpasand and Pope (2023).

2.2. Spatial and temporal scope of the study; real-urban parameters

Vehicle telematics data used in this study were collected from the roads of West Midlands in the UK for the years 2016 and 2018. They were collected from approximately 3–7 % of passenger car fleets that moved over the roads of the West Midlands in the study years. It is worth noting that, the passenger car makes

up more than 85 % of the total fleet in the West Midlands (Osei et al., 2021). Hence, this percentage contribution (3–7 %) provides a reliable representation of road transport across the studied area. For context, in 2017, over three million different vehicles travelled over the roads of the West Midlands (STATISTA, 2017). The study years of 2016 and 2018 provide a detailed understanding of road transport prior to the major interruptions caused by the COVID-19 pandemic, which was first reported in the UK in early 2020.

The method of GeoST mapping of urban mobility is used here to convert vehicle telematics data into SFAD matrices of passenger cars on GeoST-segments, see Ghaffarpasand and Pope (2023) for more details. GeoST-segments lengths vary from 15 to 150 m to cover all road features such as roundabouts, junctions, service roads, etc. Road classification follows the scheme of OpenStreetMap (OSM, www.openstreetmap.org). We present here the results for the following road designations: primary, secondary, motorways, and trunk roads, which accounted for 24.5 %, 36.8 %, 5.2 %, and 33.5 %, of the total roads studied, respectively.

The GeoST-segments are subset into 35 distinct time slots averaged over the year (2016 or 2018) comprised of the following diurnal time slots (00:00–06:59, 07:00–08:59, 09:00–11:59, 12:00–13:59, 14:00–15:59, 16:00–18:59, and 19:00–23:59) for five days a week (Mondays, Tuesdays, Fridays, Saturdays, and Sundays). It is noted that the time zone adoption was implemented, whereby Greenwich Mean Time (GMT) and British Summer Time (BST) were used as appropriate. With this adoption, the morning rush hours are, for example, between 07:00–09:00 throughout the year. The study, therefore, covers the entire temporal dimensions of passenger car transportation on urban roads, such as driving during rush or non-rush hours, weekdays, or weekends. An example figure of the GeoST-segments is shown in Fig. 1, which provides the average speed over a small area of the city of Birmingham.

Vehicle emissions and fuel consumptions are typically measured under real-world or controlled laboratory conditions using PEMS or dynamometers, respectively. A major caveat in their use is that these measurements often miss important spatial and temporal aspects of urban transport such as non-rush/rush hour, weekday/weekend effects or driving on motorways or primary roads. Their estimation in GeoST segments provides a new opportunity to consider their spatial and temporal dimensions in greater detail. Traffic activity in terms of the number of vehicles moving on the respective roads should be considered to arrive at net statistics for certain time intervals.

2.3. Vehicle specific power (VSP)

The estimated average speed and acceleration for each GeoST-segments were used to calculate matrices of vehicle fuel consumption and vehicle emissions based upon vehicle specific power (VSP). VSP was introduced by Jiménez-Palacios (1999) as the vehicle power demand at a certain point to conquer the external forces including inertial forces to maintain constant acceleration, road friction resistance force, air resistance traction, and road slope force, imposed on a moving vehicle. VSP as the instantaneous total power demand (sum of power loads resulting from aerodynamic drag forces, acceleration, rolling resistance, and hill-climbing) per vehicle mass is given by Jiménez-Palacios (1999) and Zhai et al. (2008):

$$VSP = \frac{Power\ demand}{vehicle\ mass} = \frac{P_{accl} + P_{rolling} + P_{aerodynamic} + P_{grad} + P_{internal}}{m} = \frac{\left[\overbrace{m \times a \times 1.04}^{P_{accl}} + \overbrace{R_0 + R_1 \times v}^{P_{rolling}} + \overbrace{0.5 \times C_d \times A \times \rho \times v^2}^{P_{aerodynamic}} + \overbrace{m \times g \times Grad}^{P_{grad}} + \overbrace{1.08 \times v + 2500}^{P_{internal}}\right] \times 1.08 \times v + 2500}{m} \quad (1)$$

Fig. 1. GeoST mapping of urban mobility over streets in the Ladywood area of the city of Birmingham within the West Midlands in the UK; the average speed (km/h) for 07:00–09:00 Mondays 2018.

where m is the vehicle mass and P_{accl}, $P_{rolling}$, $P_{aerodynamic}$, P_{drag}, and $P_{internal}$ are the power to accelerate the vehicle, power to overcome rolling resistance from the road, power to overcome air drag force, power to climb the road gradient, and the sum of the power required to operate auxiliary devices and losses in the transmissions, respectively. $v(\mathrm{m/s})$, $a(\mathrm{m/s^2})$, and $Grad$ are the average speed, average acceleration, and road slope, respectively; $R_0(\mathrm{N})$, $R_1(\mathrm{Ns/m})$ are road load coefficients; C_d, $A(\mathrm{m^2})$ are the aerodynamic drag coefficient and frontal surface area of the studied vehicle, respectively.

For light-duty vehicles (LDVs) 3.885 t or less, Borken-Kleefeld et al. (2018), Davison et al. (2020), and Hausberger (2003) advised some assumptions in the calculation of VSP by Eq. (1). It is assumed that the power to accelerate rotational accelerated mass is equivalent to 4 % of the power at the power for translational accelerated mass; the power losses in the transmission are equal to 8 % of the power at the driven wheels; and the power demand of auxiliaries is taken to be a fixed value of 2.5 kW. The gravity and the air density at 20 °C and 1 atm are taken to be 9.81 $\mathrm{m/s^2}$, and 1.2 $\mathrm{kg/m^3}$, respectively. The *VSP* of the LDVs (passenger cars) is then given as:

$$\mathrm{VSP}\left(\frac{\mathrm{kW}}{\mathrm{t}}\right) = \frac{2500 + (R_0 \times v + R_1 \times v^2 + C_d \times A \times 0.5 \times \rho \times v^3) \times 1.08}{m \times 1000} + 1.12 \times v \times a + \overbrace{1.08 \times v \times g \times Grad}^{slope\ part} \quad (2)$$

Borken-Kleefeld et al. (2018), Davison et al. (2020), and Hausberger (2003) proposed a set of generic coefficients of R_0, R_1, and C_dA for LDVs classified using EU_Commission (1999). Accordingly, the average generic coefficients of R_0, R_1, and C_dA for passenger cars are taken to be (157, 127), (0.95, 0.78), and (0.666, 0.598) for the (diesel cars, petrol cars), respectively.

Eq. (2) is used to calculate the spatio-temporal distribution of *VSP* by using the average speed and acceleration estimated for each GeoST-segment, see Section 2.2. The variation of *VSP* over the GeoST-segments is studied in detail by Ghaffarpasand and Pope (2023). The potential effects of road slope in Eq. (2) have previously been ignored in many emission studies which used the *VSP* in their calculations. In this study, road slope is estimated for every GeoST-segment using the method proposed by Ghaffarpasand and Pope (2023), and then two *VSP* values, which either include or not the slope part of Eq. (2), are calculated for every GeoST-segment.

2.4. Real-urban fuel consumption

According to the carbon mass balance method, fuel consumption factor (FCF) is usually estimated by the exhaustive emission factors (EFs) of CO_2, CO and total hydrocarbons (THC) through the following equation (He et al., 2022; Zhang et al., 2014a):

$$FCF\left(\frac{\mathrm{L}}{100\mathrm{km}}\right) = \frac{100}{\rho_{fuel}\left(\frac{\mathrm{g}}{\mathrm{L}}\right) \times W_c}\left(0.273EF_{CO_2}\left(\frac{\mathrm{g}}{\mathrm{km}}\right) + 0.429EF_{CO}\left(\frac{\mathrm{g}}{\mathrm{km}}\right) + 0.866EF_{THC}\left(\frac{\mathrm{g}}{\mathrm{km}}\right)\right) \quad (3)$$

where W_c is the ratio of carbon mass to total fuel mass. In the passenger car and heavy-duty emission model (PHEM), the normalised fuel consumption rate (in g/h × t) is estimated based on engine maps and vehicle longitudinal dynamics simulations (Borken-Kleefeld et al., 2018; Davison et al., 2020; Hausberger, 2003). PHEM models normalised fuel consumption over a range of driving conditions through the linear relationship between fuel consumption and engine power. Accordingly, *VSP* can be converted to fuel consumption rate (*FCR*) by a linear relationship given by Davison et al. (2020):

$$\mathrm{FCR}\left(\frac{\mathrm{g}}{\mathrm{h}}\right) = \left(M \times VSP\left(\frac{\mathrm{kW}}{\mathrm{t}}\right) + C\right) \times m \quad (4)$$

where m is the vehicle weight, and M and C are dimensionless parameters calculated from fuel flow curves for different engines. The average value of (M, C) for petrol and diesel passenger cars are (229, 552) and (204, 221), respectively. The fuel consumption rate in Eq. (4) is converted to the fuel consumption factor (FCF) using the instantaneous speed in Eq. (5):

$$FCF\left(\frac{\mathrm{g}}{\mathrm{km}}\right) = \frac{FCR\ \left(\frac{\mathrm{g}}{\mathrm{h}}\right)}{v\left(\frac{\mathrm{m}}{\mathrm{s}}\right) \times 3.6} \quad (5)$$

The fuel consumption factor is called fuel consumption (FC) hereinafter for the sake of brevity. A consequence of using a linear equation such as Eq. (4) to estimate fuel consumption is the potential for negative modelled FC values, which are physically impossible. Hence negative FC values are set to zero following Davison et al. (2020).

Eqs. (2) and (4) are used to convert spatiotemporal maps of *VSP* into the corresponding fuel consumption. To study the impact of road slope upon fuel consumption, FCs are estimated using VSPs which either consider or ignore the road slope (see Eq. (2)).

A few assumptions are required for the estimations. First, the average weight of LDVs (m in Eq. (5)) is estimated according to the published statistics of the UK vehicle market (ICCT, 2021) and fleet composition of the studied area (Fig. 2(c)). ICCT (2021) reports the average weight of brand-new cars sold in the UK (and EU) market for the past decade. Accordingly, the average cars weight (m in Eq. (5)) in the West Midlands is estimated here to be 1.878 t or 1.890 t for 2016 or 2018, respectively. The estimated fuel consumptions here are converted into the 'L/100 km' unit using the assumed densities of petrol and diesel ($\rho_{petrol} = 755\,\frac{\mathrm{kg}}{\mathrm{m^3}}, \rho_{diesel} = 838\,\frac{\mathrm{kg}}{\mathrm{m^3}}$) to compare with the published EU road statistics. The impacts of seasonality and/or regional distributions of fuel density, etc., are ignored and unified fuel densities are used here like many previous investigators such as Zhang et al. (2014a). The relative contributions of petrol and diesel cars to the fleet are estimated using the ANPR data, see next section and Fig. 2(c).

In this study, we report the relative difference between the median of the probability distribution function (PDF) of real-urban fuel consumption and official fuel consumptions. New cars in the UK are characterized by three official fuel consumptions entitled urban, extra-urban, and New European Driving Cycle (NEDC). Urban and extra-urban fuel consumptions are designed to represent fuel consumption within urban areas and non-urban areas (country roads/motorways driving), respectively. The NEDC covers almost all modes of driving. All official fuel consumptions are measured in the laboratory and under controlled conditions. On the other hand, official fuel consumption is reported according to the composition of the cars sold, for example, 48 % and 32 % of new cars sold in the UK in 2016 and 2018 were diesel, respectively. To have a reliable assessment against the official fuel consumption, we

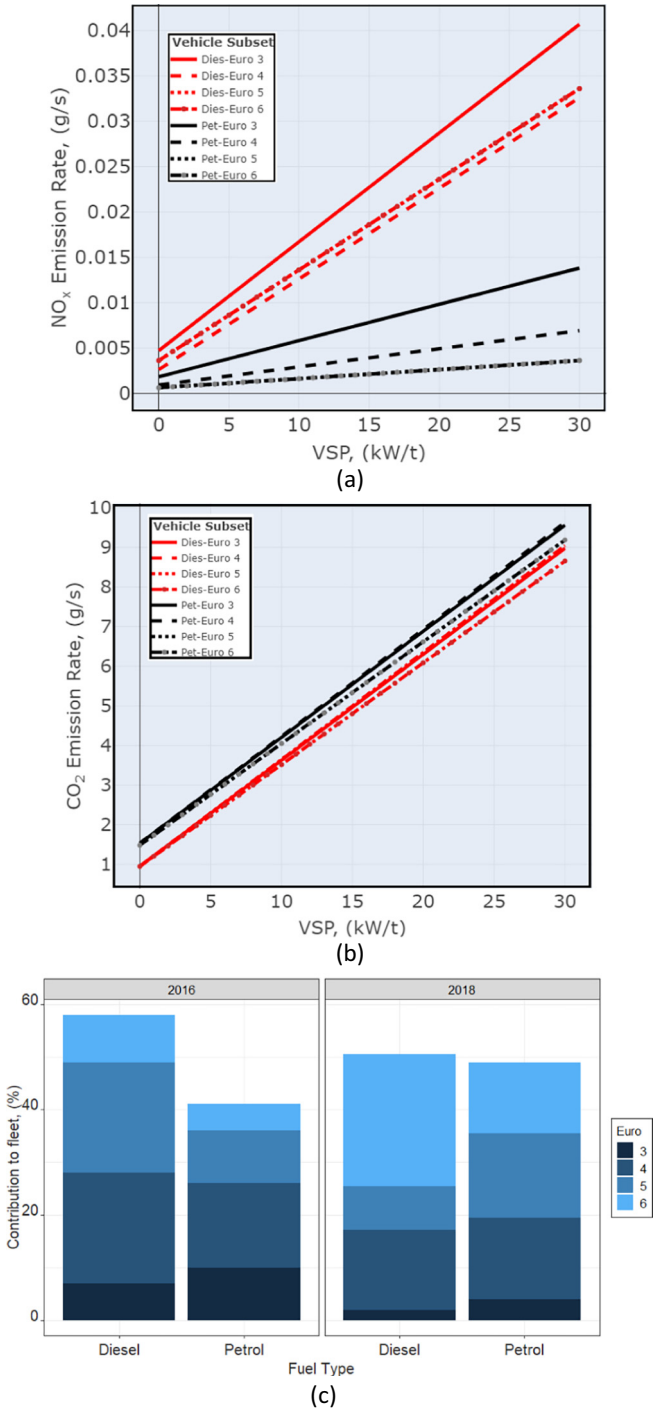

Fig. 2. The variation of exhaustive (a) NO_x and (b) CO_2 ER as a function of VSP for different vehicle subsets; (c) fleet composition of passenger cars moving over the West Midlands street network in the UK for the years 2016 and 2018.

updated those values using the relevant fleet composition considered here for 2016 and 2018. The fleet composition used here is discussed in the next section. The updated fuel consumption of brand-new vehicles in the UK market driving in under urban, extra-urban and NEDC conditions are labelled FC1, FC2, and FC3, respectively, and are shown in Fig. 3(a). The relative difference values between the median of the real-urban FCs PDF and official fuel consumptions (FC1–3 in Fig. 3(a)) are estimated using the following equation:

$$\text{Relative Difference } (\%) = \frac{MedFCAnn - FCi}{FCi} \times 100 \tag{6}$$

where *MedFCAnn* is the median value of the PDF of the real-urban fuel consumption for the whole year. The relative difference values between the median of the real-urban FCs PDF and FC1, FC2, and FC3 are shown in Fig. 3(b), (c), and (d), respectively.

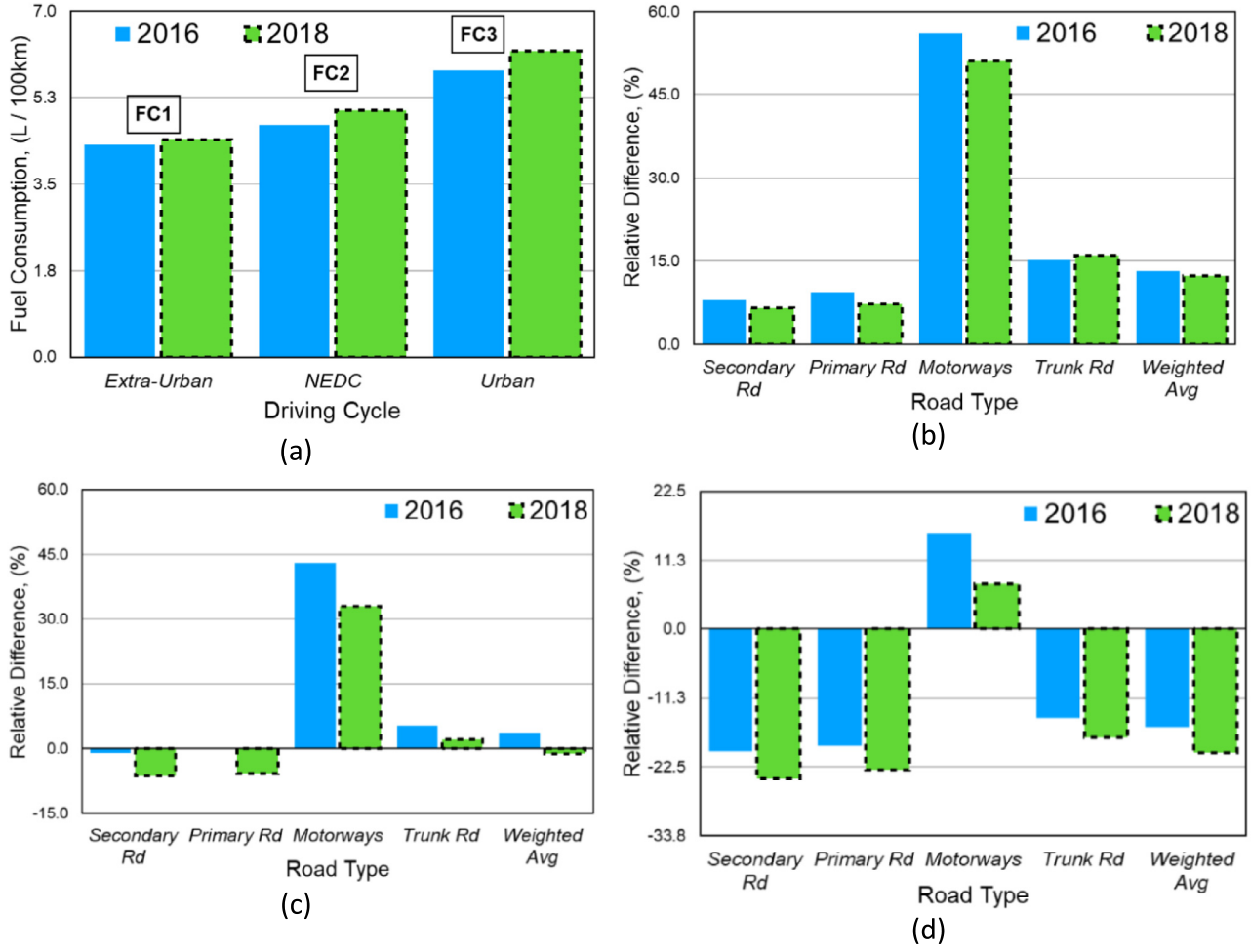

Fig. 3. (a) The average fuel consumption (FC) of brand-new vehicles in the UK vehicle market driving under extra-urban, NEDC, and urban conditions, labelled here by FC1, FC2, and FC3, respectively (ICCT, 2021); Relative difference (%) of median values for the PDF profile comparing (b) FC1, (c) FC2, and (d) FC3.

2.5. Real-urban EFs estimation; real-world EFs and fleet composition datasets

Several methods have been developed for analysing real-world EFs. Vehicle emission remote sensing systems (VERSS) assess the instantaneous ERs of moving vehicles, see for example Ghaffarpasand et al. (2020a) and Grange et al. (2019). Most VERSSs report the ratio of the concentration of pollutants including NO, NO_2, and PM to CO_2 (an indicator of fuel consumption) in the exhaust plume. The concentration ratios are then converted to fuel-based EFs (in g/kg) using recorded instantaneous CO_2 EFs, the molecular weight ratio of the studied pollutant (i.e., NO, NO_2, and PM) to CO_2 (Ghaffarpasand et al., 2023). NO_x ER is considered the sum of NO_2 and NO ERs ($NO_x = NO_2 + NO$) in most VERSS studies. Davison et al. (2020) proposed the following equations to convert fuel-based EFs into ERs and EFs.

$$\mathrm{ER}\left(\frac{g}{s}\right) = \mathrm{Fuel-based\ EF}\left(\frac{g}{kg}\right) \times \frac{FCR\left(\frac{g}{h}\right)}{3,600,000} \tag{7}$$

$$\mathrm{EF}\left(\frac{g}{km}\right) = \mathrm{Fuel-based\ EF}\left(\frac{g}{kg}\right) \times \frac{FCF\left(\frac{g}{km}\right)}{1000} \tag{8}$$

where FCR and FCF are estimated by Eqs. (4) and (5), respectively. They evaluated the method with 55 independent comprehensive PEMS measurements over a wide range of driving conditions and found a good agreement between the method and PEMS data. Davison et al. (2021) then used the method of Davison et al. (2020) to study the relationship between the instantaneous ERs and VSPs of different petrol and diesel passenger cars under different driving conditions. They studied the results of a number of UK-based VERRS and PEMS campaigns. Meanwhile, they used the fitting generalized additive models (GAMs), which are flexible enough to account for non-linear relationships between variables, to estimate the instantaneous ER-VSP for passenger cars with fuel type, engine size, Euro standards, and pollutant species. Their results show linear relationships between the NO_x and CO_2 ERs and instantaneous *VSP* of the studied vehicles. We use the (Davison et al., 2021) *VSP* parametrization of ER, with the *VSP* data from the GeoST mapping, to estimate the air pollutant (NO_x) and climate-forcing (CO_2) exhaustive emissions of vehicles under real-urban conditions.

The relationship between instantaneous *VSP* and real-world NO_x and CO_2 exhaustive ERs for different vehicle subsets (EURO Class and fuel type) are shown in Figs. 2(a) and 2(b), respectively, as provided by Davison et al. (2020) and Davison et al. (2021). The bias observed here on zero VSP values (previously observed by Davison et al., 2020 and Davison et al., 2021) may be attributed to the assumption made earlier in removing negative FCs in Eq. (4) as

well as the fitting GAMs used to predict the instantaneous ER-VSP of different car subsets. However, older vehicles, with smaller Euro numbers, have larger ERs compared to newer vehicles, and diesel cars have higher NO_x ERs compared to petrol cars. The impact of the EURO Class upon CO_2 ERs is much less when compared to the impact upon NO_x ERs.

To understand the total fleet ERs, information about fleet composition is required. To achieve a real-world picture of fleet composition across the West Midlands roads, we use automatic number plate recognition (ANPR) data provided by the local authorities that represent the wider West Midlands region (BCC, 2017; JACOBS, 2018). ANPR cameras, which are typically high-resolution infra-red (IR) cameras with ultra-bright IR LED illuminators for 24/7 covert operation, are capable of single- and double-lane imaging (with 2.9 m and 6.5 m horizontal field of view, respectively) and identification of vehicle number plates in two lanes at the same time (double-lane version) for both one-way and two-way carriageways. The data used in this study was collected from ANPR cameras installed at 36 different locations in and around Birmingham city centre. ANPR cameras are installed on the major roads and operate 24/7, the location of the cameras is reported by BCC (2017) and JACOBS (2018). The collected data are then interrogated using existing vehicle datasets, such as that provided by the UK's Driver and Vehicle Licensing Agency (DVLA) (Ropkins et al. 2017; Liu et al., 2017). From the number plate, vehicle specifications such as vehicle class, engine size, fuel type, Euro number, etc. are then obtained. The results were then anonymised and accumulated before publishing in compliance with the General Data Protection Regulation (GDPR). ANPR statistics, which are estimated by the data of tens of thousands of different vehicles, provide a reliable estimate of fleet composition.

The fleet composition of cars moving over the roads of West Midlands, subset by fuel and EURO class, for the years 2016 and 2018 is presented in Fig. 2 (c). 2018 has a greater proportion of EURO 6 and petrol vehicles in the total fleet when compared to the 2016 fleet. The ratio of diesel to petrol cars decreased from 1.41 in 2016 to 1.03 in 2018, which is a 13 % decrease in the contribution of diesel vehicles. Meanwhile, the contribution of Euro 6 vehicles is enhanced by around 63 % in 2018 when compared to 2016. This indicates fleet renewal for the period under study.

The linear relationships between *VSP* and ERs, together with the estimated fleet composition, are used to convert the spatiotemporal distribution of *VSP* into corresponding real-urban exhaustive ERs (g/s). The corresponding spatiotemporal distribution of *VSP*, see Ghaffarpasand and Pope (2023), is then used to estimate the exhaustive emission factors (EFs) under the real-urban conditions, for each GeoST-segment, through the following equation:

$$EF\left(\frac{g}{km}\right) = \frac{ER\left(\frac{g}{s}\right)}{v\left(\frac{m}{s}\right)} \times 1000 \tag{9}$$

The role of road slope is evaluated by comparing the calculated EF with and without the effect of road slope being considered, see Eq. (2), for each GeoST-segment.

3. Results and discussions

3.1. Real-rban segment-based fuel consumption

The probability distribution function (PDF) of real-urban fuel consumption for the studied time slots as well as the whole year, for both 2016 and 2018, are presented in Fig. 4(a) and (b), respectively. In Figs. 4 and 5, the official fuel consumptions are highlighted by vertical red lines and labelled FC1–3 (FC1, FC2, and FC3), see Fig. 3(a) for their values. In all the PDFs shown in Fig. 4, near unimodal distributions are observed. On secondary and primary roads, FC2 values (fuel consumption for driving under the NEDC) are very close to the median of the PDFs of real-urban FCs. For motorways, the estimated median FC values all exceed FC1–3. In Fig. 3 (b)-(d) we report the relative difference between the median of the real-urban FCs PDF and FC1–3. It can be seen that the median FC values are larger than FC3, which represents driving under urban conditions. Meanwhile, the smallest difference is observed between the median value of the PDF and FC2 values.

Except for motorways, the median values of the FC PDFs are smaller than FC2 and FC1. A significant discrepancy is observed between the real-urban FC for motorway driving and the FC1–3. This is simply attributed to higher speeds and thus higher fuel consumption on motorways. The differences between the median values of the FC PDFs and FC1–3 in 2018 are higher than that in 2016. This is attributed to the difference between real-world fleet composition in the two years (Fig. 2(c)); FC1–3 values were estimated for the brand-new vehicles. The ICCT (2021) reports a 48 % drop in the number of new brand diesel vehicles sold in the UK for 2018–2016, while Fig. 2(c) shows a 13 % drop in diesel's share of the West Midlands fleet composition.

Fig. 4 presents the impact of road slope upon fuel consumption where the solid and dashed lines correspond with FCs estimated by considering and ignoring the role of road slope, respectively, see Sections 2.2 and 2.3. The impact of road slope upon fuel consumption across the studied area is reported in Table 1.

For each specific GeoST-segment, we evaluate the relative difference in real-urban FCs estimated by ignoring and considering the role of road slope. Table 1 presents the average and standard deviations of the estimated relative differences for the studied cases. We use the same approach to study the impact of road slope on real-world NO_x and CO_2 EFs, see the next sections, and to evaluate the results estimated for the years 2016 and 2018.

Considering road slope increases fuel consumption in driving over secondary roads, primary roads, trunk roads, and motorways by (average over the studied years of 2016 and 2018) 4.9 %, 4.9 %, 4.7 % and 3.0 %, respectively. The consideration of road slope increases the estimated fuel consumption over the studied roads by the weighted averages of 4.7 % and 4.8 %, for 2016 and 2018, respectively.

The FC PDFs for secondary and primary roads are very similar. Both road types show similar diurnal patterns, with non-rush hour periods showing FC distributions shifted to higher values when compared to rush hour periods. This is attributed to the higher vehicle speeds in non-rush hours, which are translated into higher VSP and FC values. This shift to higher FC values during non-rush hour periods is more pronounced in the motorway FC distributions.

The PDF of real-urban FCs for driving on different days of the week for the years 2016 and 2018 is represented in Fig. 5(a) & (b), respectively. The results are presented here for time slots of morning rush hour (Mo_RH), non-rush hour (No_RH), and evening rush hours (Ev_RH) which correspond with the following timings: 07:00–08:59, 19:00–23:59, and 16:00–18:59, and are plotted by solid, dashed, and dotted lines, respectively. These periods did not change over the weekends and weekdays. Secondary and primary roads show similar trends for FC on different days of the week. In either road type, the weekend day profiles are distinct from the weekday profiles. There are considerable variations in the motorway FC PDFs for different days of the week. On weekdays, the peak is located towards higher FC values in non-rush hours due to higher average speeds. The morning rush hours peak moves towards higher FC values on weekends, which is likely attributed to less congestion and higher average speeds. The observed variations in the 2016 and 2018 profiles look fairly similar.

The average relative differences between the annually averaged FC over each GeoST-segment for the years 2016 and 2018 are reported in Table 2. The real-urban FC in 2018 was slightly higher than in 2016, with a weighted average of 1.4 %. This is directly attributable to the distribution of petrol and diesel vehicles for the years under study (2016 and 2018), see Fig. 2 (c). Petrol cars have usually higher fuel consumption than diesel cars. In the UK, the average fuel consumption ratio of brand-new diesel cars to petrol cars was 0.85 and 0.89 in 2016 and 2018, respectively (DFT,

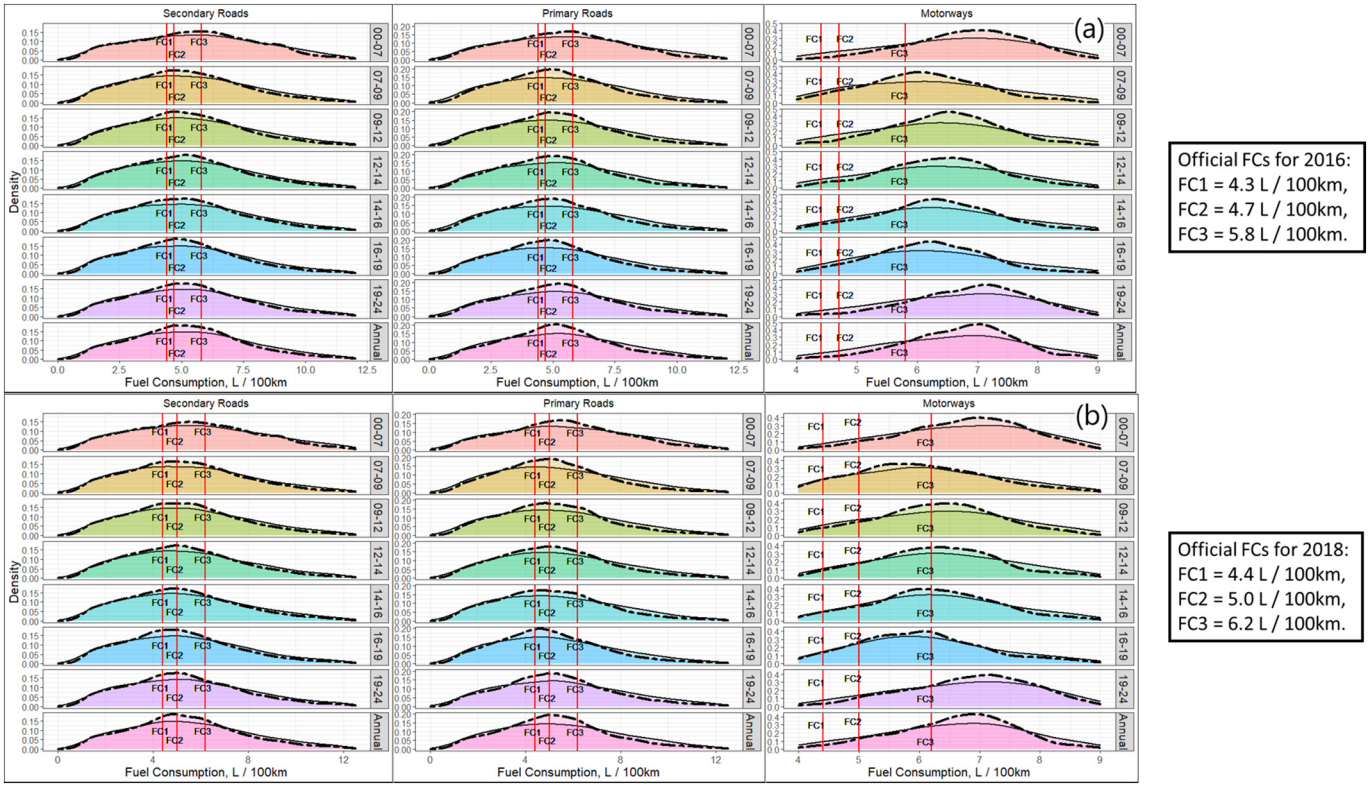

Fig. 4. The probability distribution function (PDF) of real-urban fuel consumption (FC) of cars moving over secondary roads, primary roads, and motorways within the West Midlands region of the UK, for different time slots in (a) 2016 and (b) 2018. Vertical red solid lines represent the reported FC values for the UK vehicle market and are defined in Table 1. Black and dashed solid lines stand for real-urban FCs, in which road slope is considered and ignored in their estimations, respectively.

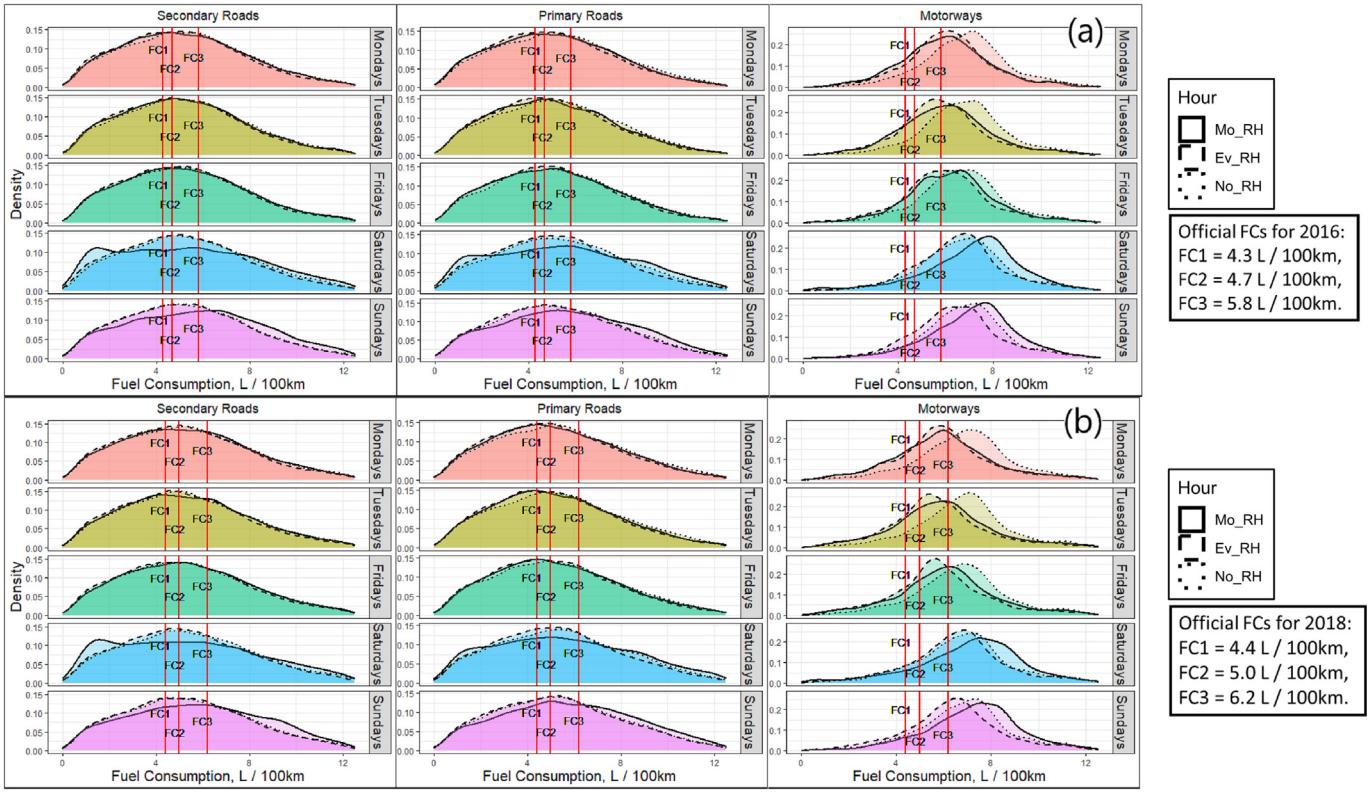

Fig. 5. The probability distribution function (PDF) of real-urban fuel consumption (FC) of cars moving over secondary roads, primary roads, and motorways of West Midlands in the UK for different days in (a) 2016 and (b) 2018. Vertical red solid lines are corresponding with the reported FC values for the UK vehicle market and are defined in Table 1. Solid, dashed, and dotted lines correspond with morning rush hours (Mo_RH, 07:00–08:59), evening rush hours (Ev_RH, 16:00–18:59), and non-rush hours (No_RH, 19:00–23:59), respectively. These periods did not change over the days of the week.

Table 1
Relative difference (%) of the fuel consumption (FC) values estimated by considering or ignoring the role of road slope, see Section 2.2. The contributions of primary, secondary, trunk, and motorways roads to the total roads studied here are used to estimate the weighted average values, see Section 2.1.

	Year	Primary roads	Secondary roads	Motorways	Trunk roads	Weighted average
Real-urban FC	2016	4.6 ± 0.4	5.4 ± 0.5	2.8 ± 0.5	4.6 ± 0.4	4.8 ± 0.4
	2018	5.2 ± 0.5	4.4 ± 0.3	3.2 ± 0.5	4.8 ± 0.4	4.7 ± 0.4
Real-urban NO_x EF	2016	4.6 ± 0.4	3.5 ± 0.3	2.2 ± 0.5	3.7 ± 0.3	3.8 ± 0.3
	2018	4.6 ± 0.4	3.7 ± 0.3	2.6 ± 0.5	3.7 ± 0.3	3.9 ± 0.3
Real-urban CO_2 EF	2016	3.6 ± 0.3	2.9 ± 0.3	1.8 ± 0.4	2.6 ± 0.2	2.9 ± 0.3
	2018	3.6 ± 0.4	3.3 ± 0.3	2.1 ± 0.4	2.6 ± 0.2	3.1 ± 0.3

Table 2
Relative differences (%) between 2018 and 2016 in fuel consumption (FC) and emission factors (EF) for NO_x and CO_2. The contributions of primary, secondary, trunk, and motorways roads to the total roads studied are used here to estimate the weighted average values, see Section 2.1.

	Primary Roads	Secondary Roads	Motorways	Trunk Roads	Weighted Average
Real-urban FC	1.8 ± 0.2	1.2 ± 0.2	−1.0 ± 0.2	1.8 ± 0.1	1.4 ± 0.2
Real-urban NO_x EF	−13.6 ± 0.1	−13.5 ± 0.1	−15.8 ± 0.1	−14.4 ± 0.1	−13.9 ± 0.1
Real-urban CO_2 EF	−0.8 ± 0.1	−0.7 ± 0.1	−2.2 ± 0.1	−2.0 ± 0.1	−1.2 ± 0.1

2023). Fig. 2(c) shows that the contribution of diesel cars decreased by 13 % and was already replaced by petrol cars for the period under study. Among the reported statistics, motorways have the least variation in FC for the studied years of 2016 and 2018. Ghaffarpasand and Pope (2023) shows that the vehicles travelled an average of 6.4 % faster on motorways in 2016 than in 2018, while they drove just 1.5 % (by average) faster on other road types. The variation in the real-urban FCs of the motorways is attributed to the contradictory effects of the average speed and fleet (petrol:diesel) composition.

3.2. Real-urban exhaustive NO_x emission

The PDFs of NO_x EFs for different time periods, for 2016 and 2018, are shown in Fig. 6(a) and (b), respectively. Fig. 6 also considers the role of

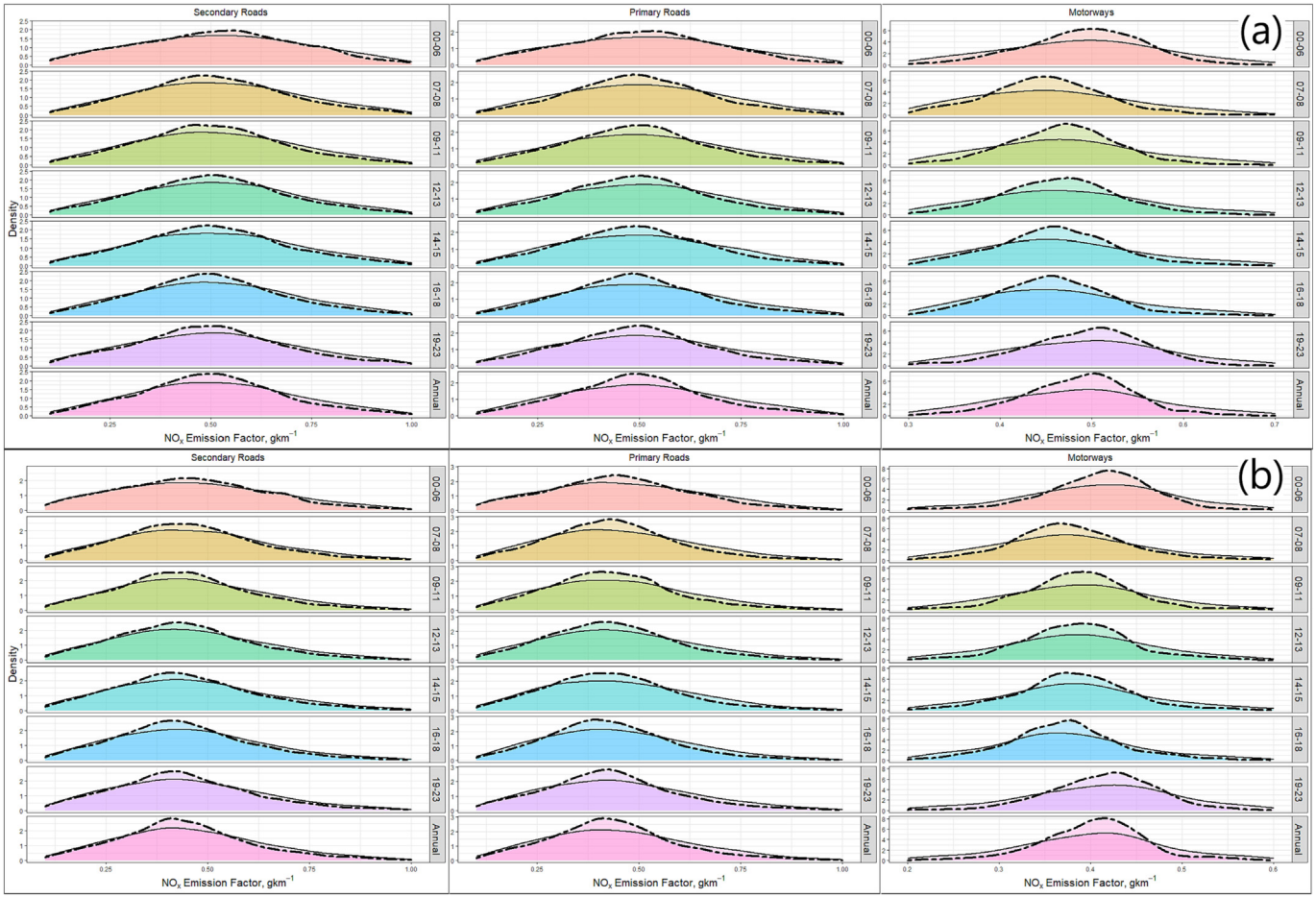

Fig. 6. The probability distribution function (PDF) of real-urban NO_x emission factor (EF) of passenger cars moving over secondary roads, primary roads, and motorways of West Midlands in the UK for different time slots in (a) 2016 and (b) 2018. Solid and dashed lines are for EFs which road slope is considered and ignored in their calculations, see Eq. (2).

Table 3
The median value (g/km) of the PDF profile of real-urban emission factors (EF) for NO_x and CO_2.

	Year	Primary Roads	Secondary Roads	Motorways	Trunk Roads
Real-urban NO_x EF	2016	0.50	0.51	0.48	0.41
	2018	0.44	0.45	0.41	0.35
Real-urban CO_2 EF	2016	157.2	160.12	205.55	192.66
	2018	154.57	157.18	202.77	190.9

road slope with the solid and dashed lines representing the PDFs of NO_x EFs estimated with and without the consideration of road slope, respectively. The role of road slope upon the estimated NO_x EFs is reported in Table 1. Considering the influence of road slope increases the estimated real-urban NO_x EFs of passenger cars moving over secondary roads, primary roads, trunk roads, and motorways by an average of 3.6 %, 4.6 %, 3.7 % and 2.4 %, respectively. The inclusion of the road slope into calculations has a weighted average impact of 3.9 % upon the estimated real-urban NO_x emission for the studied roads.

Fig. 6 shows near unimodal PDFs for NO_x EFs, which move towards higher values in non-rush hour periods. The effect is most pronounced for motorways, but also present in different road types. Higher NO_x EFs are attributed to higher speeds and accelerations, and hence higher VSPs, which are more likely to occur in non-rush hour periods. The median values are reported in Table 3, which are similar to the VERRS real-world measurements of Ghaffarpasand et al. (2020a). Ghaffarpasand et al. (2020a) analysed the real-world exhaustive EFs of around 100,000 UK-based vehicles, including vehicles in the West Midlands, measured in 2016–2017.

The impact of the day of the week upon NO_x EFs is illustrated in Fig. 7. The PDF profiles for 2018 are slightly shifted towards smaller EFs when compared with 2016. This may be attributed to two facts previously observed in Fig. 2(c) of the fleet composition of the study area. The contribution of diesel cars to the fleet in 2018 decreased by 13 % compared to 2016. The higher NO_x EFs of diesel vehicles compared to petrol vehicles have been widely discussed in the literature, see for example Ghaffarpasand et al. (2023). Meanwhile, Fig. 2(c) shows a 63 % increase in the contribution of Euro 6 vehicles in 2018 compared to 2016. This fleet renewal results in cleaner vehicles on average.

Whilst the impact of the day of travel upon the NO_x EFs seems to be marginal for primary and secondary roads, motorways show much larger variations. Fig. 7 shows the NO_x EF PDFs shift to higher EFs in non-rush hours during weekdays, while the opposite is observed on weekends. The 2018 NO_x EFs profiles are slightly damped and move to smaller EFs compared to the 2016 profiles, which are directly attributed to fleet renovation and especially the reduction of the contribution of diesel cars, see Fig. 2 (a) & (b).

The relative difference between the estimated NO_x EFs for the studied years of 2016 and 2018 is reported in Table 2. Fleet renovation reduced the estimated NO_x EFs by around 14 %. The fleet renovation has the highest impact on the NO_x EFs for motorways.

3.3. Real-urban exhaustive CO_2 emission

The PDFs of CO_2 EFs are shown in Fig. 8(a) & (b), respectively. A similar analysis to that performed on NO_x EFs is conducted with respect to: the day of the week, the hour of the day and consideration of road slope. Consideration of the road slope increased CO_2 EFs by an average of 3.1 %, 3.6 %, 2.6 % and 2 % for secondary roads, primary roads, trunk roads and motorways, respectively. Road slope has a weighted average impact of 3 % on the CO_2 EFs for driving over the studied roads.

Unsurprisingly, considering the FC PDFs, the CO_2 EF PDFs for motorways have the highest EFs and the sharpest peaks. The PDFs for secondary roads have the lowest values. The peaks of the studied profiles for secondary roads, primary roads, and motorways are located in the EF range of

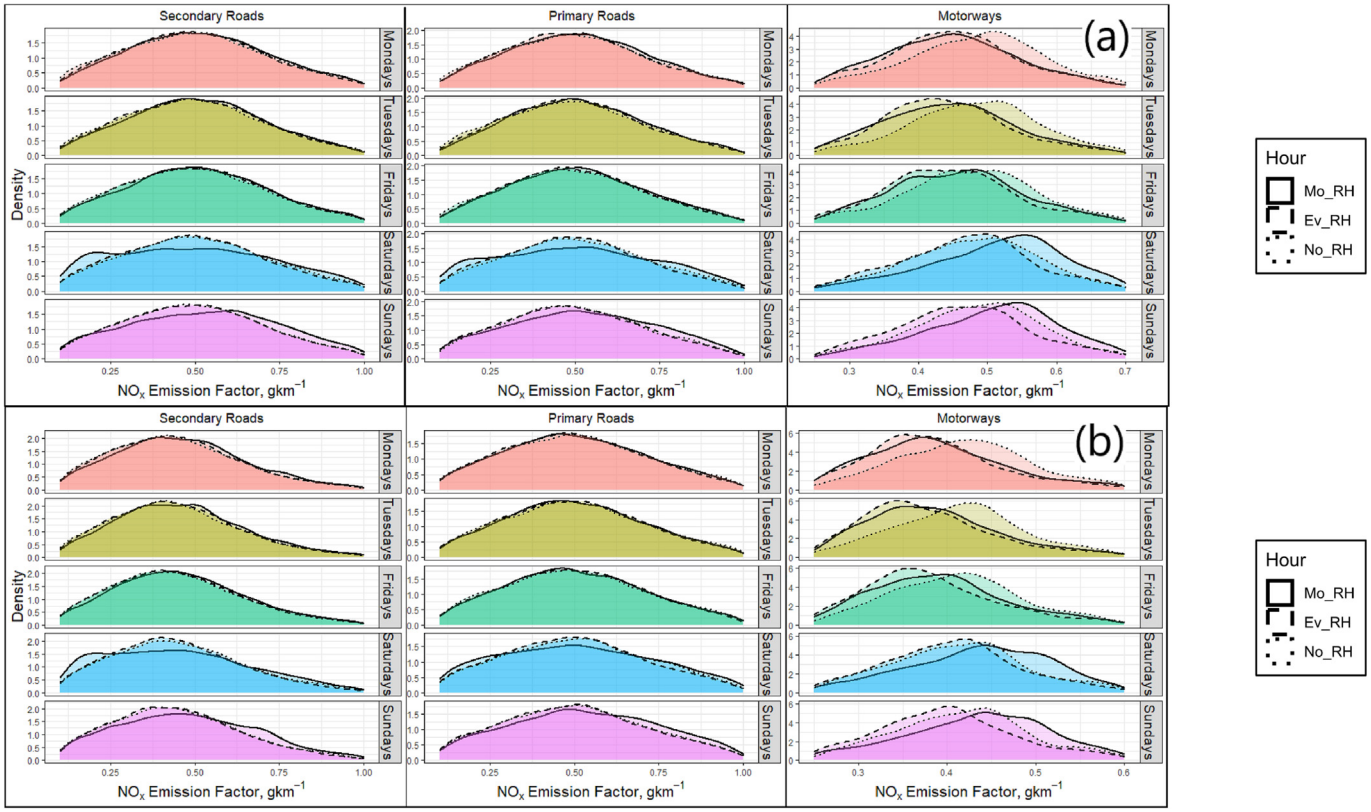

Fig. 7. The probability distribution function (PDF) of NO_x emission factor (EF) of passenger cars moving over secondary roads, primary roads, and motorways of West Midlands in the UK for different days in (a) 2016 and (b) 2018. Solid, dashed, and dotted lines correspond with morning rush hours (Mo_RH, 07:00–08:59), evening rush hours (Ev_RH, 16:00–18:59), and non-rush hours (No_RH, 19:00–23:59), respectively. These periods did not change over the days of the week.

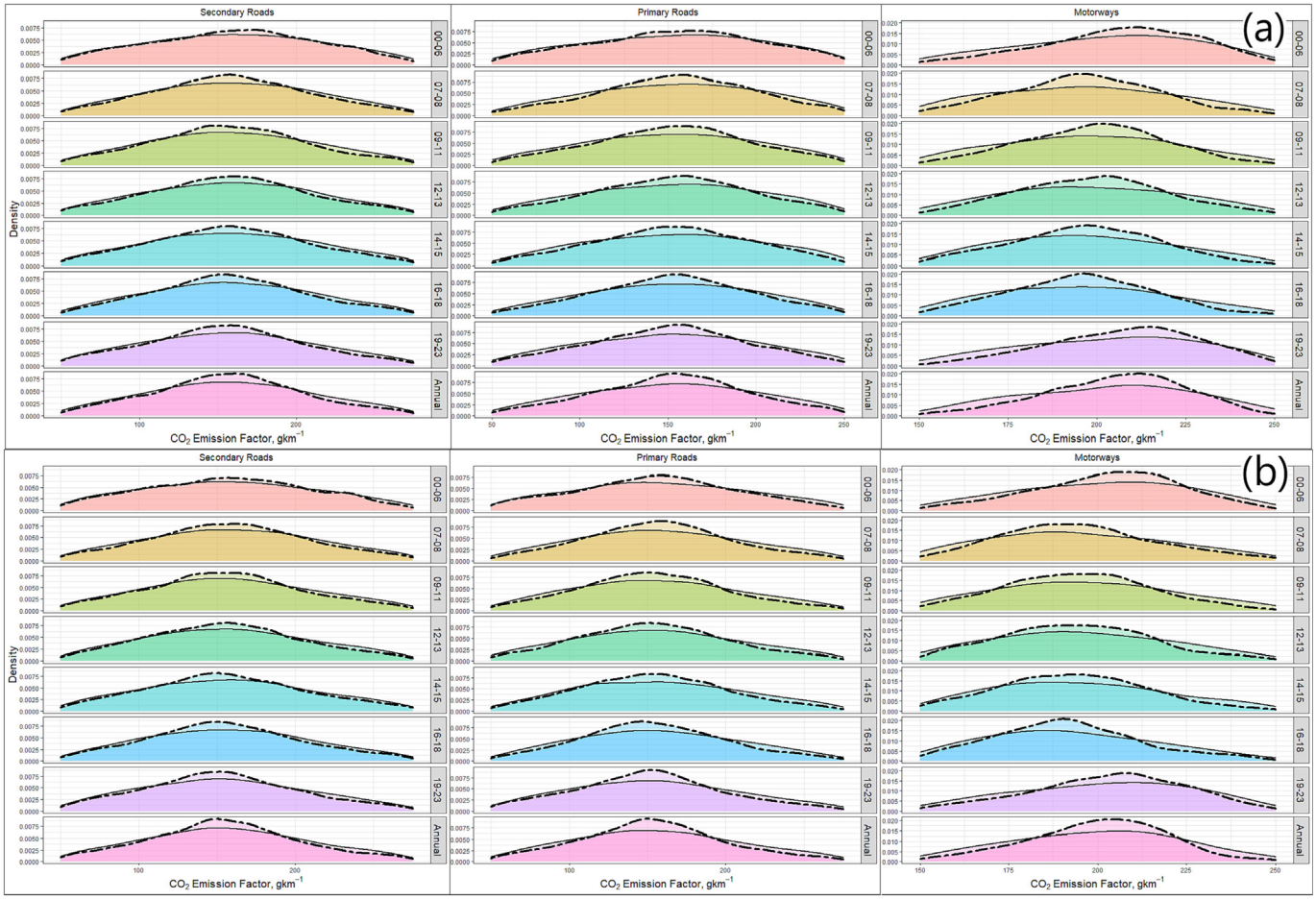

Fig. 8. The probability distribution function (PDF) of CO_2 emission factor (EF) of passenger cars moving over secondary roads, primary roads, and motorways of West Midlands in the UK for different time slots in (a) 2016 and (b) 2018. Solid and dashed lines are for EFs which road slope is considered and ignored in their calculations, see Eq. (2).

100–200 g/km, 120–170 g/km, and 180–225 g/km, respectively. The median values of the PDF profiles of real-urban CO_2 EFs, which are reported in Table 3, are in the range of 154–193 g/km. Ghaffarpasand et al. (2020a) shows that the real-world CO_2 EFs for petrol and diesel passenger cars are in the range of 150–230 g/km. The pattern of hourly variations observed in the CO_2 EFs is quite similar to the NO_x EF variations, whereby the PDFs move to higher values in non-rush hours during working days.

The impact of the day of the week upon CO_2 EFs is shown in Fig. 9. On secondary and primary roads, the impact of the day of the week is not very strong. For motorways, the day of travel has two clear impacts on CO_2 EFs. Firstly, the peak of the PDF is shifted towards higher CO_2 EFs during non-rush hours during the weekdays and rush-hours during the weekends. The CO_2 EFs for 2016 and 2018 are similar, regardless of the day of the week or time of day.

The relative differences between the annually averaged CO_2 EFs for the years 2016 and 2018 are provided in Table 2. The vehicle fleet in 2018 had slightly lower CO_2 EFs than that in 2016, which is likely due to fleet renovation and the changing ratios of different EURO classes and fuel types within the overall fleets. There were less diesels and more EURO 6 vehicles in 2018. These changes in fleet characteristics have more impact upon NO_x than CO_2 emissions.

4. Future research direction; new area in the transport environment

Vehicular fuel consumption and emissions are *scalar* transport environment parameters which are usually estimated over certain spatial and temporal resolutions. The proposed method here, however, determines new geospatial attributions to those scalar parameters and, in essence, introduces them as the new urban features. These new features can be viewed as '*fuel geo-consumption*' and '*geo-emissions*'. An example of the results of the proposed method over a very small area of the city of Birmingham, UK, is represented in Fig. 10. Fig. 10 shows an example primary school, with associated information, and the GeoST segments surrounding it. In this new paradigm, fuel geo-consumption and geo-emission are considered urban geographic features and the spatial relationships between them and the other features such as hospitals, schools, trees, traffic lights, buildings, etc., could be conceptualized/parametrized using the existing geospatial tools and platforms. Parametrizing and understanding the spatial relationships between the transport environment characteristics and other urban features will provide the future research direction of this study.

5. Conclusions

In this study, we used a new approach to convert vehicle telematics (location) data into the vehicle dynamics status (speed-time-acceleration profile) across the West Midlands road network in the UK, at (previously unattainable) spatial and temporal resolutions of 15 m and 2 h, respectively. We then used a pre-developed model, and fleet composition and real-world emission measurement datasets to evaluate transport environment characteristics of vehicular fuel consumption and emissions over highly detailed spatiotemporal contexts. We investigated the influence of factors such as road slope and time of travel on the studied characteristics of transport environment. The main results of this study are as follows:

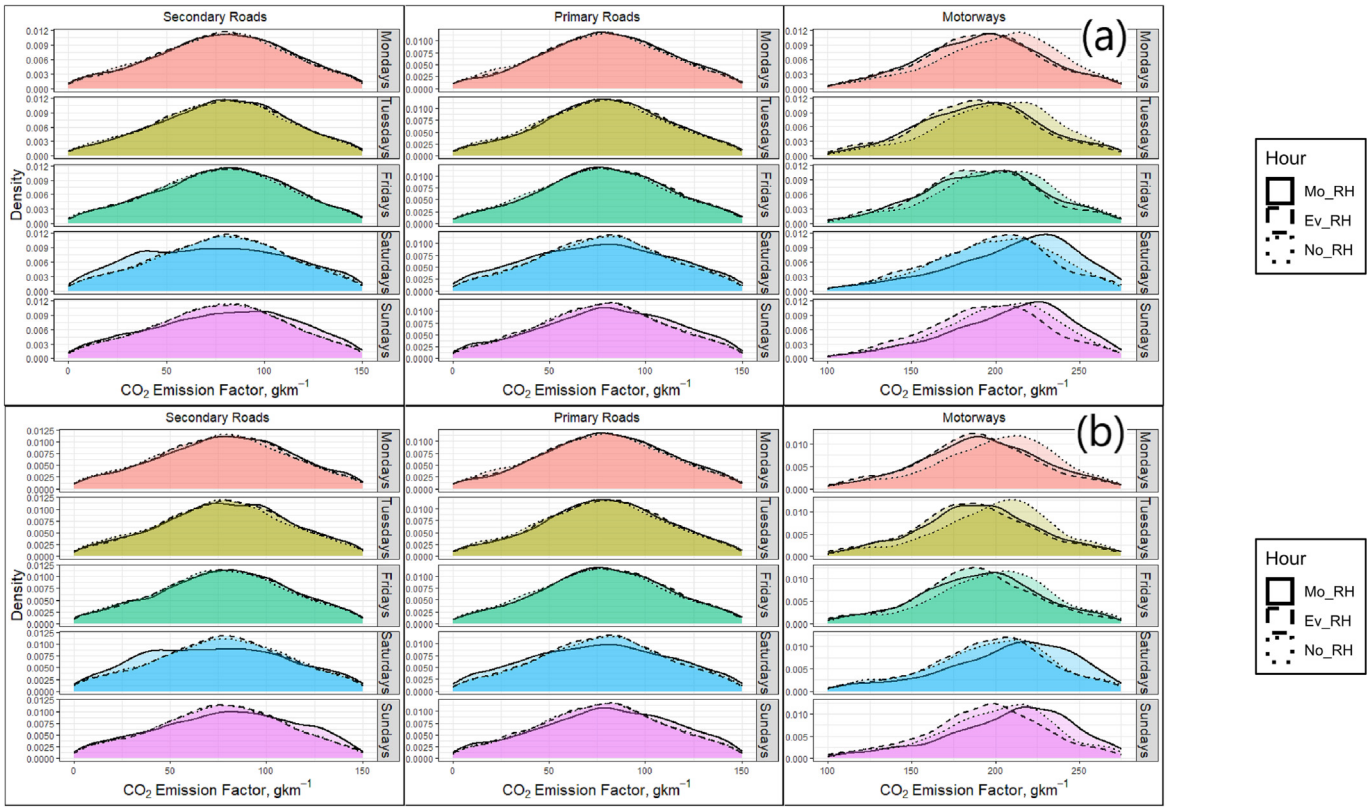

Fig. 9. The probability distribution function (PDF) of real-urban CO_2 emission factor (EF) of passenger cars moving over secondary roads, primary roads, and motorways of West Midlands in the UK for different days in (a) 2016 and (b) 2018. Solid, dashed, and dotted lines correspond with morning rush hours (Mo_RH, 07:00–08:59), evening rush hours (Ev_RH, 16:00–18:59), and non-rush hours (No_RH, 19:00–23:59), respectively. These periods did not change over the days of the week.

1. The real-urban NO_x and CO_2 EFs of on-road vehicles were reduced by a weighted average of 13.9 % and 1.2 %, respectively. This is attributed to the fleet composition development between the years 2016 to 2018, which led to a 63 % and 13 % increase and decrease in the contribution of Euro 6 and diesel vehicles to the total vehicle fleet, respectively.
2. The on-road vehicles in 2018 have 1.4 % higher real-urban fuel consumption compared to 2016, which is explained by the increasing contribution of petrol cars.
3. An average of 2–5 % increase is observed in the estimated FC, and CO_2 and NO_x EFs by considering the role of road slope in the

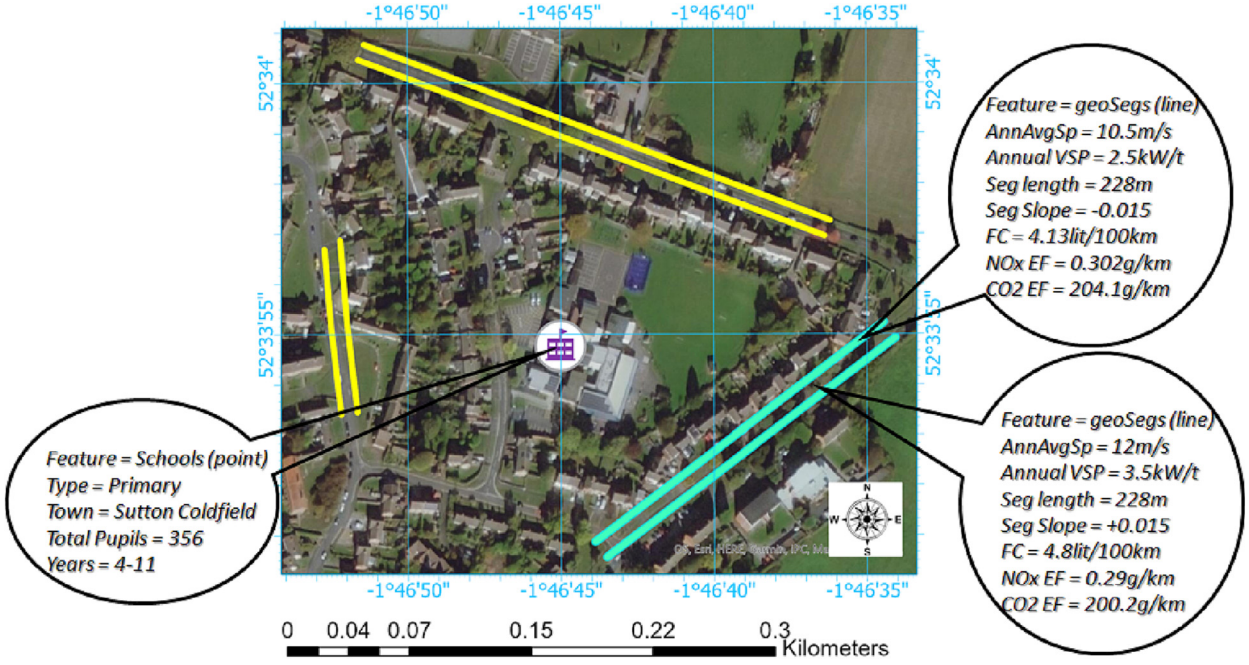

Fig. 10. A small area of the city of Birmingham, West Midlands, UK, with corresponding geo-emissions and fuel geo consumption for Mondays, 9–11, 2016. All attributed data are reported here for the year 2016.

calculations. The least impacts are observed for motorway driving.
4. The PDFs of the FC and NO_x and CO_2 EFs are typically near-unimodal. The exact PDF profile is dependent upon time of the day, and day of week, in addition to the type of road under investigation.

The new GeoST approach to the estimation of FC and EFs allows for a deeper understanding of how urban design affects air pollution and climate change. Going forward, the approach detailed in this paper allows urban planners to consider how to optimize roads with other urban features, such as schools, hospitals, shops, malls, etc.

CRediT authorship contribution statement

Omid Ghaffarpasand: Conceptualization, Methodology, Data curation, Formal analysis, Visualization, Writing – original draft. **Francis D. Pope:** Conceptualization, Investigation, Supervision, Writing – review & editing.

Data availability

Data will be made available on request.

Declaration of competing interest

The authors declare that they have no known competing financial interests or personal relationships that could have appeared to influence the work reported in this paper.

Acknowledgement

We gratefully acknowledge the support and funding from the Natural Environment Research Council, UK (NERC) via the WM-Air (NE/S003487/1), and the Met Office via the SPF Clean Air Program funding of the DUKEMS project.

References

BCC, 2017. Birmingham Clean Air Zone Feasibility Study. Birmingham City Council.
Bhatti, A.H.U., Kazmi, S.A.A., Tariq, A., Ali, G., 2021. Development and analysis of electric vehicle driving cycle for hilly urban areas. Transp. Res. Part D: Transp. Environ. 99, 103025.
Borken-Kleefeld, J., Hausberger, S., Mcclintock, P., Tate, J., Carslaw, D., Bernard, Y., Sjödin, Å., Jerksjö, M., Gentala, R., Alt, G.-M., Tietge, U. & Fuente, J. 2018. Comparing emission rates derived from remote sensing with PEMS and chassis dynamometer tests.
Chen, S., Bekhor, S., Yuval, Broday, D.M., 2016. Aggregated GPS tracking of vehicles and its use as a proxy of traffic-related air pollution emissions. Atmos. Environ. 142, 351–359.
Coelho, S., Ferreira, J., Rodrigues, V., Lopes, M., 2022. Source apportionment of air pollution in European urban areas: lessons from the ClairCity project. J. Environ. Manag. 320, 115899.
Davison, J., Bernard, Y., Borken-Kleefeld, J., Farren, N.J., Hausberger, S., Sjödin, Å., Tate, J.E., Vaughan, A.R., Carslaw, D.C., 2020. Distance-based emission factors from vehicle emission remote sensing measurements. Sci. Total Environ. 739, 139688.
Davison, J., Rose, R.A., Farren, N.J., Wagner, R.L., Murrells, T.P., Carslaw, D.C., 2021. Verification of a national emission inventory and influence of on-road vehicle manufacturer-level emissions. Environ. Sci. Technol. 55, 4452–4461.
DFT, 2023. Energy and environment: Data tables (ENV). Fuel Consumption (ENV01). Department for Transport.
EU 2019. Transport. European Union.
EU_Commission 1999. Regulation (EEC) no 4064/89 Merger Procedure Article 6(1)(b) Non-Opposition, Technical Report *European* Commission.
Gately, C.K., Hutyra, L.R., Peterson, S., Sue Wing, I., 2017. Urban emissions hotspots: quantifying vehicle congestion and air pollution using mobile phone GPS data. Environ. Pollut. 229, 496–504.
Ghaffarpasand, O. & Pope, F. 2023. Telematics data for geospatial and temporal mapping of urban mobility: new insights into the travel characteristics and vehicle specific power. Preprint for the time being.
Ghaffarpasand, O., Beddows, D.C.S., Ropkins, K., Pope, F.D., 2020a. Real-world assessment of vehicle air pollutant emissions subset by vehicle type, fuel and EURO class: new findings from the recent UK EDAR field campaigns, and implications for emissions restricted zones. Sci. Total Environ. 734, 139416.
Ghaffarpasand, O., Khodadadi, M., Majidi, S., Rozatian, A.S.H., 2020b. Multi-elemental characterization of PM0.4–0.7 and PM1.1–2.1 in the ambient air of Isfahan (Iran) complemented by the speciation of Mn and Cr using SR-XANES. Aerosol Science and Engineering 4, 124–136.
Ghaffarpasand, O., Talaie, M.R., Ahmadikia, H., Khozani, A.T., Shalamzari, M.D., 2020c. A high-resolution spatial and temporal on-road vehicle emission inventory in an Iranian metropolitan area, Isfahan, based on detailed hourly traffic data. Atmospheric Pollution Research 11, 1598–1609.
Ghaffarpasand, O., Talaie, M.R., Ahmadikia, H., Talaiekhozani, A., Shalamzari, M.D., Majidi, S., 2020d. On-road performance and emission characteristics of CNG-gasoline bi-fuel taxis/private cars at the roadside environment. Atmospheric Pollution Research 11, 1743–1753.
Ghaffarpasand, O., Talaie, M.R., Ahmadikia, H., Khozani, A.T., Shalamzari, M.D., Majidi, S., 2021. Real-world assessment of urban bus transport in a medium-sized city of the Middle East: driving behavior, emission performance, and fuel consumption. Atmospheric Pollution Research 12, 113–124.
Ghaffarpasand, O., Burke, M., Osei, L.K., Ursell, H., Chapman, S., Pope, F.D., 2022. Vehicle telematics for safer, cleaner and more sustainable urban transport: a review. Sustainability [Online] 14.
Ghaffarpasand, O., Ropkins, K., Beddows, D.C.S., Pope, F.D., 2023. Detecting high emitting vehicle subsets using emission remote sensing systems. Sci. Total Environ. 858, 159814.
Google Maps. 2023. Use eco-friendly routing on your Google maps app [online]. Google. Available: https://support.google.com/maps/answer/11470237?hl=en [Accessed].
Grange, S.K., Farren, N.J., Vaughan, A.R., Rose, R.A., Carslaw, D.C., 2019. Strong temperature dependence for light-duty diesel vehicle NOx emissions. Environ. Sci. Technol. 53, 6587–6596.
Hausberger, S. 2003. Simulation of real world vehicle exhaust emission.
He, L., You, Y., Zheng, X., Zhang, S., LI, Z., Zhang, Z., Wu, Y., Hao, J., 2022. The impacts from cold start and road grade on real-world emissions and fuel consumption of gasoline, diesel and hybrid-electric light-duty passenger vehicles. Sci. Total Environ. 851, 158045.
Hu, J., Wu, Y., Wang, Z., Li, Z., Zhou, Y., Wang, H., Bao, X., Hao, J., 2012. Real-world fuel efficiency and exhaust emissions of light-duty diesel vehicles and their correlation with road conditions. J. Environ. Sci. 24, 865–874.
Hu, R., Zhang, F., Peng, Z., Pei, Y., 2022. The NOx emission characteristics of gasoline vehicles during transient driving cycles. Transp. Res. Part D: Transp. Environ. 109, 103386.
Huang, Y., Meng, S., 2019. Automobile insurance classification ratemaking based on telematics driving data. Decis. Support. Syst. 127, 113156.
Hung, W.T., Tong, H.Y., Lee, C.P., Ha, K., Pao, L.Y., 2007. Development of a practical driving cycle construction methodology: a case study in Hong Kong. Transp. Res. Part D: Transp. Environ. 12, 115–128.
Ibarra-Espinosa, S., Ynoue, R.Y., Ropkins, K., Zhang, X., de Freitas, E.D., 2020. High spatial and temporal resolution vehicular emissions in south-east Brazil with traffic data from real-time GPS and travel demand models. Atmos. Environ. 222, 117136.
ICCT, 2021. European vehicle market statistics. The International Council on Clean Transportation (ICCT), pocketbook 2019/20, 60-65.
JACOBS, 2018. City Center Data Collection Report. Birmingham City Council.
Jia, X., Wang, H., Xu, L., Wang, Q., Li, H., Hu, Z., Li, J., Ouyang, M., 2021. Constructing representative driving cycle for heavy duty vehicle based on Markov chain method considering road slope. Energy and AI 6, 100115.
Jiménez, J.L., 1998. Understanding and Quantifying Motor Vehicle Emissions with Vehicle Specific Power and TILDAS Remote-Sensing. (Ph.D. thesis)Massachusetts Institute of Technology, Cambridge, Massachusetts.
Jiménez-Palacios, J. L. Understanding and quantifying motor vehicle emissions with vehicle specific power and TILDAS remote sensing. 1999.
Kancharla, S.R., Ramadurai, G., 2018. Incorporating driving cycle based fuel consumption estimation in green vehicle routing problems. Sustain. Cities Soc. 40, 214–221.
Liu, Y., Lu, K., Ma, Y., Yang, X., Zhang, W., Wu, Y., Peng, J., Shuai, S., Hu, M., Zhang, Y., 2017. Direct emission of nitrous acid (HONO) from gasoline cars in China determined by vehicle chassis dynamometer experiments. Atmos. Environ. 169, 89–96.
Marabete, M., Dalla Chiara, B., Maino, C., Spessa, E., 2022. Electrified road transport through plug-in hybrid powertrains: compliance by simulation of CO2 specific emission targets with real driving cycles. Transportation Research Interdisciplinary Perspectives 15, 100651.
Mjøsund, C.S., Hovi, I.B., 2022. GPS data as a basis for mapping freight vehicle activities in urban areas – a case study for seven Norwegian cities. Res. Transp. Bus. Manag. 100908.
Molina Campoverde, P.A., Rivera Campoverde, N.D., Morales Espinoza, J.E., Rodriguez Fernandez, G.M., Novillo, G.P., 2022. Influence of the road slope on NOx emissions during start up. Materials Today: Proceedings 49, 8–15.
Osei, L.K., Ghaffarpasand, O., Pope, F.D., 2021. Real-world contribution of electrification and replacement scenarios to the fleet emissions in West Midland boroughs, UK. Atmosphere [Online] 12.
Pradhan, R.P., 2019. Investigating the causal relationship between transportation infrastructure, financial penetration and economic growth in G-20 countries. Res. Transp. Econ. 78, 100766.
Ropkins, K., Defries, T.H., Pope, F., Green, D.C., Kemper, J., Kishan, S., Fuller, G.W., LI, H., Sidebottom, J., Crilley, L.R., Kramer, L., Bloss, W.J., Stewart Hager, J., 2017. Evaluation of EDAR vehicle emissions remote sensing technology. Sci. Total Environ. 609, 1464–1474.
Soto, F., Dorado-Vicente, R., Torres-Jiménez, E., Cruz-Peragón, F., 2023. Prediction of emissions and performance from transient driving cycles using stationary conditions: study of advanced biofuels under the ETC test. Case Studies in Thermal Engineering 41, 102618.
STATISTA, 2017. Number of Licensed Cars in the West Midlands, England between 2000 and 2017. Statista.
Walker, G., Manson, A., 2014. Telematics, urban freight logistics and low carbon road networks. J. Transp. Geogr. 37, 74–81.
Wang, X.-C., Klemeš, J.J., Dong, X., Fan, W., Xu, Z., Wang, Y., Varbanov, P.S., 2019. Air pollution terrain nexus: A review considering energy generation and consumption. Renew. Sust. Energ. Rev. 105, 71–85.

Zhai, H., Frey, H.C., Rouphail, N.M., 2008. A vehicle-specific power approach to speed- and facility-specific emissions estimates for diesel transit buses. Environ. Sci. Technol. 42, 7985–7991.

Zhang, S., Wu, Y., Liu, H., Huang, R., Un, P., Zhou, Y., Fu, L., Hao, J., 2014a. Real-world fuel consumption and CO2 (carbon dioxide) emissions by driving conditions for light-duty passenger vehicles in China. Energy 69, 247–257.

Zhang, S., Wu, Y., Liu, H., Huang, R., Yang, L., Li, Z., Fu, L., Hao, J., 2014b. Real-world fuel consumption and CO2 emissions of urban public buses in Beijing. Appl. Energy 113, 1645–1655.

Zhang, R., Fujimori, S., Dai, H., Hanaoka, T., 2018. Contribution of the transport sector to climate change mitigation: insights from a global passenger transport model coupled with a computable general equilibrium model. Appl. Energy 211, 76–88.